Reviews in Mathematical Physics
Vol. 17, No. 7 (2005) 769–792

World Scientific
www.worldscientific.com

WETTING PHENOMENA AND CONSTANT MEAN CURVATURE SURFACES WITH BOUNDARY

RAFAEL LÓPEZ

Departamento de Geometría y Topología,
Universidad de Granada, 18071 Granada, Spain
rcamino@ugr.es

Received 20 October 2004
Revised 08 June 2005

In a microscopic scale or microgravity environment, interfaces in wetting phenomena are usually modeled by surfaces with constant mean curvature (CMC surfaces). Usually, the condition regarding the constancy of the contact angle along the line of separation between different phases is assumed. Although the classical capillary boundary condition is the angle made at the contact line, configurations also occur in which a Dirichlet condition is appropriate. In this article, we discuss those with vanishing boundary conditions, such as those that occur on a thin flat portion of a plate of general shape covered with water. In this paper, we review recent works on the existence of CMC surfaces with non-empty boundary, with a special focus on the Dirichlet problem for the constant mean curvature equation.

Keywords: Mean curvature; Dirichlet problem; maximum principle.

Mathematics Subject Classification 2000: 53A10, 35J65, 35Q35, 76B45

1. Modeling the Morphology of the Interface

Phase changes in states of equilibrium are influenced by the presence of surfaces and interfaces. An interface is the zone existing between two immiscible substances. The understanding of the shape of interfaces is a major objective in numerous scientific activities, such as engineering, chemical industry, nanotechnology and medicine. A typical example of interface occurs when we deposit an amount of liquid on a planar surface. We assume that no chemical reaction occurs between the two materials and that these are homogeneous. In a state of mechanical equilibrium, the droplet attains a fixed position. Wetting is the study of how that droplet spreads out on the substrate. Surface tension between two phases explains the local forces which tend to minimize its interfacial area, being responsible both for the shape and the deformation that the droplet takes. These forces of cohesion have a limited reach and their effects are detectable within a small molecular radius; they will be greater in solids, lower in liquids and almost negligible in gas. Besides liquid droplets on a solid substrate, interfaces appear in a variety of settings: capillarity

when a tube is dipped in a reservoir of liquid; a liquid droplet floating on another immiscible liquid; the shape formed by the liquid when it adheres to a wall; a droplet of liquid trapped between two closely-spaced horizontal plates. In wetting and adhesion phenomena, experimentalists are interested in the physical/chemical properties of materials and the morphology of the interfaces that explains, to a certain degree, these characteristics. Mean curvature of these interfaces plays a special role in the shapes and morphologies.

The classical mathematical model used for equilibrium configurations is essentially based on the classical Young–Laplace–Gauss equation. We consider a solid substrate (S) whose properties do not change in a gas environment (G). When one deposits a certain amount V of a liquid (L) — a droplet — on the substrate (S), the energies of this system consist of three types: a free surface energy of the (LG) interface $\mathcal{S}$, an adhesion energy of the liquid (L) over the substrate and a volume constraint. Denote $\mathcal{S}_{IJ}$ the area of the interface between phases I and J and γ_{IJ} the corresponding interfacial energy density. The equilibrium state of the liquid droplet corresponds with those configurations that are stationary values of the total interfacial free energy as given by $E = \gamma_{LG}\mathcal{S}_{LG} + \gamma_{LS}(\mathcal{S}_{LS} - \mathcal{S}_{GS}) + (P_G - P_L)V$. The pressure term $P_G - P_L$ is included to fulfil the constraint on the volume. In order to minimize the energy E, one considers an interface $\mathcal{S}$ of arbitrary shape and performs small displacements of this interface that ensure that the (GLS) phase stays within the substrate surface. Interfacial shapes of minimal free energy are found from the requirement that all variations of the free energy, which are of first order in the displacements, must vanish. The theoretical model that describes the interface $\mathcal{S}$ is then expressed by the equation

$$P_L - P_G = \gamma_{LG}\left(\frac{1}{R_1} + \frac{1}{R_2}\right).$$

Here R_1 and R_2 denote the principal curvature radii that define the normal curvature of the interface $\mathcal{S}$ in two orthogonal planes containing the unit normal vector at each point of the interface. The mean curvature at a point of a smooth surface is defined by $H = \frac{1}{2}\left(\frac{1}{R_1} + \frac{1}{R_2}\right)$. Thus one obtains the Young equation which measures the excess pressure across $\mathcal{S}$ [72, 35]:

$$P_L - P_G = 2H\gamma_{LG}. \tag{1.1}$$

Complete derivations can be found in [1, 19, 52, 39, 15]. If one assumes the existence of gravity (for example, for sufficiently large droplets), we must add in the expression of E the potential energy $\rho\int_L h$, where ρ is the difference between the gravities of the (L) and (G) phases, and h is the height above a reference level. We do not consider this term since we will focus on wetting structures when gravity is absent or for which the effects of gravity are small and can be ignored.

In the case that both γ_{LG} and $P_G - P_L$ are constant, the interface $\mathcal{S}$ is a *constant mean curvature surface*. Constant mean curvature surfaces are obtained from a variational argument as follows. First, the contact line C of the physical

system is the region of contact between the gas, liquid and solid phases. If D is an open subset of the (u^1, u^2)-plane, we parametrize $\mathcal{S}$ by a one-to-one smooth function $\mathbf{x} : D \to \mathbb{R}^3$, where $\mathbf{x}_1, \mathbf{x}_2$ are two independent tangent vectors. The notation $\mathbf{x}_i$ means the differentiation with respect to u^i. Moreover, we assume that $\mathbf{x}_{|\partial D}$ is a parametrization of the curve C. We orient the surface by the unit normal vector $N = (\mathbf{x}_1 \times \mathbf{x}_2)/|\mathbf{x}_1 \times \mathbf{x}_2|$. Take a variation $\mathbf{x}(t) : D \to \mathbb{R}^3$, $t \in \mathbb{R}$, of $\mathcal{S} := \mathbf{x}(0)(D)$ by surfaces $\mathcal{S}_t = \mathbf{x}(t)(D)$ with the same boundary C and enclosing the same volume as $\mathcal{S}$. Since the energy is proportional to the interfacial area, let us measure the area $A(t)$ of $\mathcal{S}_t$. In equilibrium, we seek critical points of $A(t)$ under the constraint that the volume is constant (in fact, surface tension creates a tendency to minimize area). But a straightforward computation leads to $A'(0) = -2\int_{\mathcal{S}} H(\partial_t \mathbf{x}(t))_{t=0} \cdot N \, \mathrm{d}\mathcal{S}$, where H is the mean curvature of $\mathcal{S}$. Thus, if we impose $A'(0) = 0$ for any such variations, we conclude that H is a constant function, that is, *CMC surfaces are critical points of the area functional under variations enclosing a fixed volume and spanning a fixed boundary.*

On the other hand, and from the theory of differential geometry, the intrinsic geometry of the $\mathcal{S}$ interface is expressed in terms of two quadratic differential forms. The first fundamental form is the metric tensor $\mathbf{G} = [g_{ij}] = \mathbf{x}_i \cdot \mathbf{x}_j$. The second fundamental form is the curvature tensor defined by

$$[h_{ij}] = N \cdot \mathbf{x}_{ij} = -N_i \cdot \mathbf{x}_j$$

and the mean curvature H is then given by

$$H = \frac{1}{2} \text{ trace } \mathbf{G}^{-1}[h_{ij}]. \tag{1.2}$$

In order for the surface $\mathbf{x}(u^1, u^2)$ to have constant mean curvature H, the value H in (1.2) is the same at all points on $\mathcal{S}$.

Examples of CMC surfaces are spheres and cylinders. If the radius is R, the mean curvature with respect to the inward orientation is $H = \frac{1}{R}$ and $H = \frac{1}{2R}$ respectively. If the interface is planar, $R_1, R_2 \to \infty$ and so, the difference of pressure vanishes, that is, the pressure on both sides of the interfaces agrees. Surfaces with zero mean curvature at each point are called *minimal surfaces*. As guides to the theory of minimal surfaces, see [53, 54].

2. Physical Configurations with Prescribed Boundary

The structure of the contact line C is determined by the intermolecular forces between the substrate and the molecules within the fluid phase. Due to homogeneity of our models, the thermodynamic equilibrium between the three interfaces concludes that the contact angle θ which the liquid-gas interface $\mathcal{S}$ meets the substrate (S) is *constant* along the curve C. This angle θ is determined by the Gauss equation

$$\gamma_{GS} - \gamma_{LS} = \gamma_{LG} \cos\theta. \tag{2.1}$$

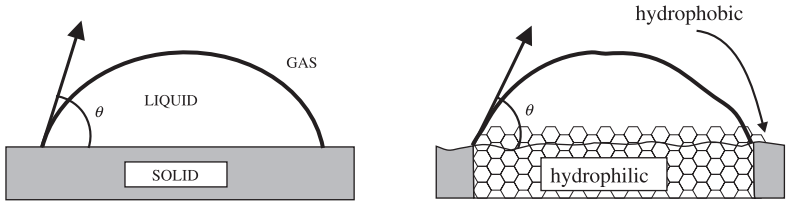

Fig. 1. (a) A droplet in a state of equilibrium and with homogeneous phases. The angle θ is constant according to Eq. (2.1); (b) Hysteresis in a droplet in equilibrium on a heterogeneous substrate. The contact angle changes along the liquid-air-solid phase.

See [18] and Fig. 1(a). Thus the contact angle depends on the surface tensions between the different phases and so, it is an intrinsic property of the system.

The combination of Eqs. (1.1) and (2.1) is of great importance because it allows the computations of the interface tensions of solid-liquid and solid-gas by an indirect method. There exist a number of measurement techniques to determine the surface tension [1]. Following Eqs. (1.1) and (2.1), the experimentalist tries to obtain an approximate knowledge of the morphology of the interface thanks to the use of photographic/optical techniques, where accuracy depends on the precision of the instruments used. Usually one assumes a certain symmetry of the interface, such as, for example, the interface being rotationally symmetric, since this simplifies the computations. Once the shape of the meniscus and the angle θ have been obtained, numerical integration allows the determination of the value of H. There is an extensive literature on capillarity. We refer readers to [14, 34, 20] and references therein. For the rest of this article, we shall assume that the effect of gravity is negligible, for example, in a microgravity environment or microscopic scale. Therefore, our interfaces are modeled by CMC surfaces.

However, it is difficult to achieve ideal conditions in wetting experiments due to a variety of factors, for example, contamination, impurity, viscosity and volatility in the liquid; roughness, chemical heterogeneity, dirtiness and change of the hydrophilic degree in the substrate. As a consequence, the constancy of the contact angle θ is dropped and Eq. (2.1) is not fulfilled. This phenomenon is known as *hysteresis* and the value of the contact angle θ varies in a certain range, see Fig. 1(b). In the bibliography, one can find a great number of formulations to justify or to complete Eq. (2.1), see [27, 57, 64, 20]. Precisely, the difference between θ with the expected angle according to Eq. (2.1) is used as a test to measure the degree of cleanliness and roughness of the substrate.

We focus on those configurations with a Dirichlet condition and without any assumption on the angle of contact. For example, consider a hydrophobic flat substrate Π with a hydrophilic domain Ω. An amount of liquid placed on this substrate will tend to wet only the domain Ω by forming a droplet that covers the whole domain Ω. In addition, if we assume non-ideality both in the liquid as in

the substrate, the hysteresis phenomenon appears along the contact line. In such situations, the interface $\mathcal{S}$ is a CMC surface with *prescribed boundary* $C = \partial\Omega$. The interest lies in how the geometry of the boundary line C will be manifested in the shape of the drop. As an immediate question: *does the droplet inherit the symmetries of* C?

In contrast to the physical experiments, the geometric structure of the space of CMC surfaces with boundary is not well known. The simplest case of boundary, that is, when C is a circle, shows the experience/theory contrast. A physicist *assumes* that a droplet deposited on a round disc substrate adopts a spherical shape, whereas a mathematician allows other possible configurations, for example, a doughnut-shaped droplet. Indeed, the following is still unsolved:

Conjecture. *Let* $\mathcal{S}$ *be a CMC surface with a circular boundary. If one of the following conditions holds, then* $\mathcal{S}$ *is a spherical cap*:

(1) $\mathcal{S}$ *is a topological disc.*
(2) $\mathcal{S}$ *has no self-intersections* (*embedded*).

Our experience says that when we dip a round wire into a soap solution and then blow through it, the real morphologies are spherical bubbles. However, in 1991, Kapouleas proved the existence of CMC surfaces spanning a circle with holes and self-intersections [28].

Although we have considered the case where the boundary is planar, one can pose other configurations, something of which has recently been dealt with by experimentalists: fluids deposited in ring-shaped domains [36], liquids whose boundaries are constrained in two or three spheres [37, 63, 69], and probably, the most studied case, liquid bridges between parallel planes and wedges. See, for example, [33, 50, 55, 58].

Now, a brief comment on the structure of the rest of the text. The material of this review is not organized as a sequence of "Theorem" and "Proof", but we present it as a continuum of the results that we want to point out. On the other hand, this article is far from being a survey on CMC surfaces in $\mathbb{R}^3$, for example, we do not treat the techniques on construction of complete or closed CMC surfaces, or the capillarity theory. Our aim is to show that this field is sufficiently active to be attractive to the reader.

3. The Dirichlet Problem of the CMC Equation

If the domain Ω is wetted by a not too large amount of liquid, the contact angle θ does not exceed $\pi/2$ and it is natural to think that the projection of $\mathcal{S}$ is one-to-one on Ω. Therefore, a first attempt is to describe these droplets as graphs on Ω. Let $\Omega \subset \mathbb{R}^2$ be a smooth domain. Given a real number H and a continuous function ϕ on $\partial\Omega$, the corresponding Dirichlet problem for the CMC equation consists of

finding a function $f \in C^2(\Omega) \cap C(\bar{\Omega})$ that satisfies

$$\operatorname{div}(Tf) = -2H \quad \text{in } \Omega, \quad Tf = \frac{Df}{\sqrt{1+|Df|^2}}, \tag{3.1}$$

$$f = \phi \quad \text{along } \partial\Omega. \tag{3.2}$$

Geometrically, H is the mean curvature of the surface $z = f(x, y)$, whose boundary is $C = \text{graph } \phi$. The orientation N assumed on the graph points downward, that is, $N = (Df, -1)/\sqrt{1+|Df|^2}$. If $\phi = 0$, then the boundary of the surface is the curve $\partial\Omega$.

Equation (3.1) is an elliptic second order partial differential equation in two coordinates. Although it is not a linear equation, the difference of the two solutions of the same equation is, and we can apply the Hopf maximum principle ([26], [21, Theorem 9.2]). In geometric terms, we have:

Theorem 3.1 (Tangency Principle). *Let $\mathcal{S}_1$ and $\mathcal{S}_2$ be two surfaces in $\mathbb{R}^3$ with the same constant mean curvature. Suppose that they are tangent at a common interior point p and the Gauss maps N_1 and N_2 agree at p. If $\mathcal{S}_1$ lies locally above $\mathcal{S}_2$ at p with respect to $N_1(p) = N_2(p)$, then $\mathcal{S}_1$ and $\mathcal{S}_2$ coincide in a neighborhood of p. The same holds if p is a common boundary point with the extra hypothesis that $\partial\mathcal{S}_1$ and $\partial\mathcal{S}_2$ are tangent at p.*

In contrast, Eq. (3.1) cannot be solved analytically in most cases, even if $\mathcal{S}$ is a surface of revolution (in such a case, solutions involve elliptic integrals, see Eq. (3.6)). Thus it is necessary to apply numerical methods to determine the shape of the interface. Recently, several techniques have been developed, for example, the application MESH at the GANG (Center for Geometry, Analysis, Numerics and Graphics) at the University of Massachusetts [25], and the software *Surface Evolver* designed by Brakke [6].

The general technique employed in the solvability of the Dirichlet problem is the method of continuity. We briefly explain this technique with some detail ([10, 21]). Consider H a fixed real number. For each $t \in [0, 1]$, we pose the family of Dirichlet problems

$$(P_t): \quad \begin{cases} \operatorname{div}(Tu_t) = -2tH & \text{in } \Omega, \\ u = \phi & \text{along } \partial\Omega. \end{cases}$$

Define the set

$$J = \{t \in [0,1]; \text{there exists a solution } u_t \text{ of } (P_t)\}.$$

In this setting, a solution of (3.1) and (3.2) exists provided one shows that $1 \in J$. For this purpose, we shall prove that J is a non-void, open and closed subset of $[0, 1]$, and hence, $J = [0, 1]$. Let us prove first that $0 \in J$, that is, there exists a minimal surface with the same boundary value ϕ on $\partial\Omega$. In general, this solution is obtained from the very theory of minimal surfaces and, at first, this difficulty is not easily overcome (but if $\phi = 0$, then $u = 0$ is an immediate solution). In the second step,

we prove that J is open in $[0,1]$. Consider $\tau \in J$ and we will see that the Dirichlet problem (P_t) can be solved for each t in a certain interval around τ. Denote by Σ_t the graph corresponding to u_t and define a map $h : C_0^{2,\alpha}(\Sigma_\tau) \to C_0^{\alpha}(\Sigma_\tau)$ taking each v onto the mean curvature function of the normal graph on Σ_τ corresponding to the function v:

$$h(v) = \text{mean curvature of } (p \mapsto x(p) + v(p)N(p)),$$

where $x : \Sigma_\tau \hookrightarrow \mathbb{R}^3$ is the inclusion map. The linearization of h is the Jacobi operator of Σ_τ, namely,

$$L(v) = \Delta v + |\sigma|^2 v,$$

where Δ is the Laplace–Beltrami operator in Σ_τ and σ is its second fundamental form. Here L is a self-adjoint linear elliptic operator with trivial kernel, since

$$L\langle N, \vec{a}\rangle = 0 \quad \text{and} \quad \langle N, \vec{a}\rangle < 0, \tag{3.3}$$

where N is the orientation on Σ_t and $\vec{a} = (0,0,1)$. Hence, and using the implicit function theorem for Banach spaces, h is locally invertible. This shows that there exists a solution u_t of (P_t) for values of t around τ.

Finally, it remains to be proved that J is closed in $[0,1]$. The Schauder theory reduces the question to establish *a priori* C^0 and C^1 estimates of each solution u_t of (P_t) independent of t, that is, it suffices to prove that there exists a constant M independent of t such that

$$\sup_\Omega |u_t|, \quad \sup_\Omega |Du_t| \le M.$$

The value of $|u_t|$, that is, the height of Σ_t is controlled by a universal constant. Let us consider $\mathcal{S}$ a graph of a function u defined in a domain Ω. Assume that the mean curvature H is constant. Denote $x : \mathcal{S} \hookrightarrow \mathbb{R}^3$ the inclusion map of $\mathcal{S}$. From (3.3),

$$\Delta(H\langle x, \vec{a}\rangle + \langle N, \vec{a}\rangle) = -2(H^2 - K)\langle N, \vec{a}\rangle,$$

where K is the Gaussian curvature of $\mathcal{S}$. If $\mathcal{S}$ is a graph, $\langle N, \vec{a}\rangle < 0$ and consequently, the function $H\langle x, \vec{a}\rangle + \langle N, \vec{a}\rangle$ is subharmonic. Maximum principle implies that its maximum is attained at a certain boundary point and thus,

$$|u| = |\langle x, \vec{a}\rangle| \le \sup_{\partial\Omega} |\phi| + \frac{1}{|H|}. \tag{3.4}$$

In particular: *If $\mathcal{S}$ is a graph with constant mean curvature H and planar boundary, the height of $\mathcal{S}$ from the boundary plane is at most* $1/|H|$. This result appears first in [66] and has been recently generalized for unbounded domains [62].

Let us return to our setting. As a consequence of the maximum (or tangency) principle, $u_0 < u_t < u_1 \le \sup_{\partial\Omega} |\phi| + 1/|H|$.

Now we seek *a priori* estimates for $|Du_t|$. By the expression of N in terms of Du_t, we know

$$\langle N, \vec{a}\rangle = -\frac{1}{\sqrt{1+|Du_t|^2}}. \tag{3.5}$$

But Eq. (3.3) tells us that $\Delta\langle N, \vec{a}\rangle \geq 0$ and so, the maximum of $\langle N, \vec{a}\rangle$ is attained at a boundary point of $\partial\Omega$. By combining with (3.5), we conclude

$$\sup_{\Omega} |Du_t| = \sup_{\partial\Omega} |Du_t|.$$

At this moment, and for each particular case of domain Ω, we shall need suitable surfaces as barriers to compare the slope of the graph of u_t along its boundary: if $|Du| \to \infty$, $N \to \pm\vec{a}$. Usually, they are pieces of rotational CMC surfaces.

Rotational surfaces in the Euclidean space with constant mean curvature are known as Delaunay surfaces. Consider a surface $\mathcal{S} = \{(r(s)\cos\theta, r(s)\sin\theta, s); s \in I, \theta \in \mathbb{R}\}$ obtained by rotation with respect to the z-axis of the generating curve $(r(s), 0, s)$, $s \in I$ and $r(s) > 0$ on I. Then the mean curvature H satisfies $1 + r'^2 - rr'' = 2H(1+r'^2)^{3/2}$. Because

$$\frac{d}{ds}\left(Hr^2 - \frac{r}{\sqrt{1+r'^2}}\right) = 0,$$

a first integral yields

$$Hr^2 - \frac{r}{\sqrt{1+r'^2}} = c \tag{3.6}$$

for a constant c. Anyway, the function r cannot be completely integrated, but it involves elliptic integrals. Delaunay discovered that the profile curve is the trace of a focus of a conic that rolls on the axis of revolution (the z-axis) [11]. Besides the catenoid ($H = 0$), Delaunay surfaces are unduloids and nodoids, and the limit cases, spheres and cylinders. See Fig. 2.

It is possible to assure the existence of the Dirichlet problem for a few cases of domains Ω. Recall that not every value of H is allowed, because a simple integration

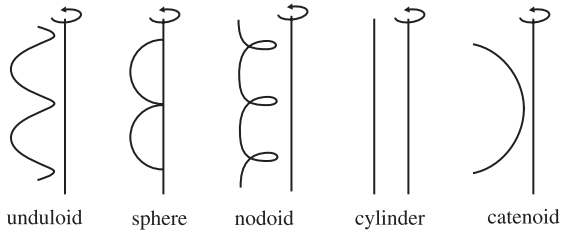

Fig. 2. Profiles curves of Delaunay surfaces.

of (3.1) together with the divergence theorem implies that

$$2|H| < \frac{\text{length}(\partial\Omega)}{\text{area}(\Omega)}. \tag{3.7}$$

When Ω is a round disc, the only CMC graphs are (small) spherical caps.

When Ω is a bounded convex domain, the classical result of the existence for Eq. (3.1) and an arbitrary boundary condition is due to Serrin [65]:

> *If the curvature κ of $\partial\Omega$ with respect to the inner orientation satisfies $0 < 2|H| < \kappa$, then for an arbitrary smooth function ϕ on $\partial\Omega$, there exists a unique solution of* (3.1) *with $f = \phi$ along $\partial\Omega$.*

However, for droplets resting on planar substrates, that is, for $\phi = 0$ on $\partial\Omega$, one expects that the range of possible H is bigger, as it happens when Ω is a round disc. Some recent results have been obtained:

Theorem 3.2. *Let Ω be a bounded convex domain. If one of the following assumptions holds, then there is a solution of Eq.* (3.1) *for $f = 0$ along $\partial\Omega$:*

(1) $0 < |H| < \kappa$, *where κ is the curvature of $\partial\Omega$* [43].
(2) *length* $(\partial\Omega) < \sqrt{3}\pi/|H|$ [49].
(3) *area* $(\Omega) < \pi/(2H^2)$ [46].
(4) Ω *is included in a strip of width* $1/|H|$ [44].

In this theorem, pieces of spheres and cylinders are used as barriers since they fit well with the convexity of the domain Ω. We briefly present the proof of item (1) as a demonstration of our machinery (this result was proved under the stronger condition $\kappa > 2|H|/\sqrt{3}$ in [56]).

Since the boundary condition is $\phi = 0$ on $C := \partial\Omega$, the function $u = 0$ is the solution of (P_0). Next, we know that J is an open set of $[0, 1]$ and that we have C^0 bounds for u_t, $t \in [0, 1]$. We only need to control the slope of u_t along C. Without loss of generality, we may assume that H is positive and $u_t > 0$ on Ω. Let $\rho, \eta > 0$ be real numbers such that $H < 1/\rho < 1/\eta < \kappa$. Let us take concentric circles Γ_ρ, Γ_η of radii ρ and η, respectively, in the same plane $\Pi = \{x_3 = 0\}$ that contains C. Let us move both circles until C lies within the disc that bounds Γ_η in Π: this is possible due to the choice of η and the convexity of C. Take a hemisphere S_ρ of radius ρ supported on Π and whose boundary is Γ_ρ. Let us descend S_ρ until the intersection with Π is Γ_η and denote S_η the piece of S_ρ over Π (a spherical cap). The surface S_η is a graph on Π whose mean curvature is $1/\eta$, with $1/\eta > H$. See Fig. 3. The tangency principle implies that Σ_t lies in the bounded domain determined by $S_\eta \cup \Pi$. Because $1/\eta < \kappa$, and by rolling Γ_η along C, it is possible to move S_η by horizontal translations in such a way that ∂S_η touches *each* point of C. The tangency principle prohibits any contact between S_η and Σ_t before S_η touches Σ_t at a boundary point. In addition, the slope of Σ_t is less than that of S_η: this slope depends only on η but not on t, which provides an *a priori* estimate of $|Du_t|$ on $\partial\Omega$.

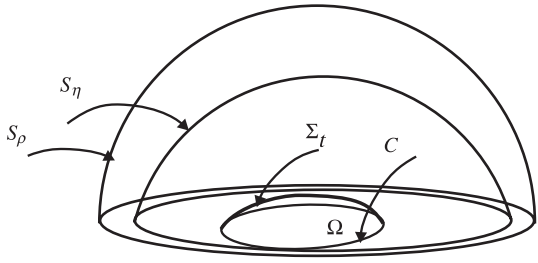

Fig. 3. Proof of Theorem 3.2.

The results of Theorem 3.2 in terms of the size of the domain Ω are not optimal, as shown if Ω is a round disc. Other results of the existence of graphs on convex domains, though somewhat too complicated to state here, are obtained in [12, 60]. However, little is known when the boundary is not convex, and even less so, when C is not a planar curve. See also [65, 16, 47] for results of the existence of radial CMC graphs whose boundary is included in a given sphere.

For non-bounded domains, the first examples that appear are half-cylinders, where the domain Ω is an infinite strip. Finn suggested in [13] that the half-cylinder of radius $1/(2|H|)$ is the only graph with constant mean curvature H in a strip of width $1/|H|$. Collin [9] showed that other different solutions exist: given a strip B, let us take a convex function ϕ and we place two copies of the graph of ϕ over each straight line of ∂B. He showed the existence of a solution f of (3.1) on B such that $f = \phi$ along ∂B. For a general unbounded convex domain Ω, the author has proved:

Theorem 3.3 ([44]). *Let Ω be an unbounded convex domain. The necessary and sufficient condition to solve the Dirichlet problem* (3.1) *for $f = 0$ along the boundary is that Ω lies in a band of width $\frac{1}{|H|}$.*

For non-bounded domains, we use the Perron method to obtain the desired solution: see [9, 10, 21] and for an example in the same context. We describe how this technique works by proving Theorem 3.3. Without loss of generality, let us assume $H > 0$. Denote $L_H(u) = \operatorname{div}(Tu) + 2H$. Let v be a continuous function in Ω and $D \subset \Omega$ a closed disc. We denote by $\bar{v}$ the unique solution of the Dirichlet problem $L_H(\bar{v}) = 0$ in D satisfying the condition $\bar{v} = v$ on ∂D. The existence of the function $\bar{v}$ is assured by the Serrin result since the radius of D is less than $1/(2H)$. We define the function $M_D(v)$ in Ω as

$$M_D(v) = \begin{cases} \bar{v}(p), & p \in D, \\ v(p), & p \in \Omega \backslash D. \end{cases}$$

The function v is a *subsolution* in Ω if $v \leq M_D(v)$ for every disc $D \subset \Omega$. If, in addition, $v \leq 0$ along ∂D, we say that v is a *subfunction* relative to 0. The class F of all subfunctions relative to 0 is a non-empty set and is closed in the sense that $M_D(v) \in F$ provided that $v \in F$.

If the band B where Ω lies is $\{(x,y) : -1/(2H) < y < 1/(2H)$, consider the half-cylinder $z(x,y) = \sqrt{1/(4H^2) - y^2}$ and $Z = z_{|\Omega}$. Let us define $F^* = \{v \in F; 0 \leq v \leq Z\}$, with similar properties to F, and

$$u = \sup\{v; v \in F^*\} = \sup\{M_D(v); v \in F^*, D \subset \Omega\}.$$

The Perron method shows that the function u is a solution of $L_H(u) = 0$ in Ω. Finally, it remains to be proved that u is continuous on $\bar{\Omega}$ and that it takes the value 0 along the boundary. The fact that u is continuous in Ω is a consequence of the Harnack principle. The latter statement is achieved by using pieces of half-cylinders as barrier surfaces at the boundary points. Taking $p \in \partial\Omega$, it is possible to find a quarter of cylinder $\mathcal{Q}$ with the same mean curvature as the graph $\mathcal{S}$ of u in such a way that $\mathcal{S}$ lies between $\mathcal{Q}$ and B. The maximum principle together with the convexity of the domain shows that u takes the value 0 in each boundary point of Ω, proving the theorem.

In this result, as in [9], the barriers have been pieces of cylinder. Other results of the existence can be given in a stripped domain or non-convex domains. We shall need the following definition.

Definition 3.4. A domain $\Omega \subset \mathbb{R}^2$ is said to satisfy an *exterior ρ-circle condition* if it is possible to roll a circle C_ρ of radius ρ with $C_\rho \subset \mathbb{R}^2 \setminus \Omega$ and C_ρ touches each point of $\partial\Omega$. In the same way, if $f : \mathbb{R} \to \mathbb{R}$ is a smooth function, we say that f satisfies an exterior ρ-condition if one of the domains $\mathbb{R}^2 \backslash \text{graph}\,(f)$ satisfies an exterior ρ-circle condition.

See Fig. 4. Now we can state the following:

Theorem 3.5 ([45, 59]). *Let $H > 0$ and let B be a strip of width $1/H$.*

(1) *Let $\Omega \subset B$ be a domain that satisfies an exterior ρ-circle condition. There exists a number $h_\rho > 0$, depending on H, Ω and ρ, such that if $H < h_\rho$, Eq.* (3.1) *has a solution u, with $u = 0$ along $\partial\Omega$.*
(2) *Let $\Omega \subset B$ be an infinite strip and f satisfying an exterior ρ-condition. There exists a number $h^\rho > 0$, depending on f, H, Ω and ρ such that if $H < h^\rho$, Eq.* (3.1) *has a solution u, with $u = f$ along $\partial\Omega$.*

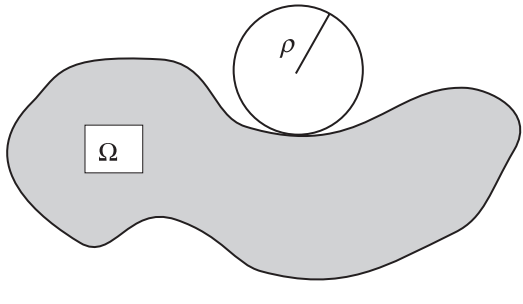

Fig. 4. A domain Ω satisfying an exterior ρ-circle condition.

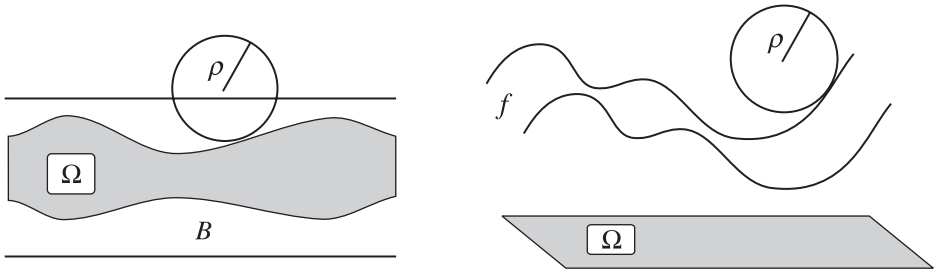

Fig. 5. Theorem 3.5, cases (1) and (2).

Examples of domains appear in Fig. 5. The proof of this result is similar to that in Theorem 3.3, except that the barrier is a suitable piece of nodoid adequate to our setting.

Let us finally pose some open problems related to the subject of this section.

Q1 In view of Theorem 3.2, some of the results are not optimal. For example, does the Dirichlet problem have a solution when length $(\partial\Omega) < 2\pi/|H|$ or when area $(\Omega) < \pi/H^2$?

Q2 It has been proved in (3.4) that the height of a graph with constant mean curvature H spanning a planar boundary is less than $1/|H|$. Hemispheres show that this bound is optimal, but we do not know whether the bound $1/|H|$ is achieved for other configurations of boundary, even in the case that $\partial\Omega$ is a convex curve.

4. The Effect of the Boundary in the Morphology of the Droplet

In this section, we shall describe the effect of the geometry of the boundary in the shape of the whole surface. Consider $\mathcal{S}$ a CMC surface with non-empty boundary $\partial\mathcal{S}$. Let Y be a variational field in Euclidean three-space $\mathbb{R}^3$. Then the first variation formula of the area $|A|$ of the surface $\mathcal{S}$ along Y gives

$$\delta_Y|A| = -2H\int_{\mathcal{S}}\langle N, Y\rangle\, d\mathcal{S} - \int_{\partial\mathcal{S}}\langle Y, \nu\rangle\, ds,$$

where ν and ds represent, respectively, the inner unit vector along $\partial\mathcal{S}$ and the length-arc element of $\partial\mathcal{S}$. Let us fix a vector $\vec{a} \in \mathbb{R}^3$ and consider Y the vector field of translations in the direction of $\vec{a}$. Since Y generates isometries of $\mathbb{R}^3$, the first variation of A is 0. Then

$$2H\int_{\mathcal{S}}\langle N, \vec{a}\rangle\, ds + \int_{\partial\mathcal{S}}\langle \nu, \vec{a}\rangle\, ds = 0. \tag{4.1}$$

The first integral changes into an integral on the boundary as follows. The divergence of the field $Z_p = (p \wedge \vec{a}) \wedge N$, $p \in \mathcal{S}$, is $-2\langle N, \vec{a}\rangle$. The divergence theorem,

together with (4.1), yields

$$\int_{\partial\mathcal{S}} \langle \nu, \vec{a} \rangle \, ds + H \int_{\partial\mathcal{S}} \langle \alpha \times \alpha', \vec{a} \rangle \, ds = 0, \tag{4.2}$$

where α is a parametrization of $\partial\mathcal{S}$ such that $\alpha' \wedge \nu = N$.

This equality is known as the "balancing formula" or "flux formula" (see [32] for the embedded case). It is a conservation law in the sense of Noether that reflects the fact that the area (the potential) is invariant under the group of translations of Euclidean space. On the other hand, the formula can be viewed as the physical equilibrium between the forces of the surface tension of $\mathcal{S}$ that act along its boundary with the pressure forces that act on the bounded domain by $\partial\mathcal{S}$. More generally, if we cut $\mathcal{S}$ into a collection of opens, then the surface tension along the cuts and the pressure through the caps must balance.

If the boundary $\partial\mathcal{S}$ lies in the plane $\Pi = \{x \in \mathbb{R}^3; \langle x, \vec{a} \rangle = 0\}$, for $|\vec{a}| = 1$, then $\langle \alpha \times \alpha', \vec{a} \rangle$ is simply the support function of the boundary. Therefore

$$2H\bar{A} = \int_{\partial\mathcal{S}} \langle \nu, \vec{a} \rangle \, ds, \tag{4.3}$$

where $\bar{A}$ is the area of the domain that bounds $\partial\mathcal{S}$. This formula holds for an arbitrary *immersed* surface. See [48]. Thus, given a closed curve $C \subset \mathbb{R}^3$, the value H of the possible mean curvature of surfaces whose boundary is C cannot be imposed, but is determined by the geometry of the boundary curve C:

$$|H| < \frac{\text{length}(C)}{2\text{area}(\Omega)}. \tag{4.4}$$

This generalizes (3.7). In particular, *if C is a circle of radius $R > 0$, a necessary condition for the existence of a surface spanning C with constant mean curvature H is that $|H| \leq 1/R$* [22].

For the rest of this section, we point out some recent aspects in the theory of CMC surfaces with boundary.

4.1. *Small CMC surfaces*

Classically, there are two ways to obtain CMC surfaces spanning a prescribed closed curve C: the Plateau and isoperimetric problems. Let us recall both problems here. Given a fixed Jordan curve $C \subset \mathbb{R}^3$, the Plateau problem asks for an immersed CMC surface spanning C. In order to avoid complicated topology of the surfaces, one restricts to consider immersions $X : \bar{D} \to \mathbb{R}^3$ from the closed unit disc $\bar{D} \subset \mathbb{R}^2$ such that $\partial X(D) = C$. For this, one minimizes the functional

$$\text{Area} \; - 2H \cdot \; \text{Volume}$$

in a suitable class of surfaces with the same boundary C. Also, we must assure that there exists such a surface with a finite area. The techniques employed come from the functional analysis. This viewpoint was initiated by Douglas but it was from

the 1950s to the present when it became an active field for a number of authors like Brézis, Coron, Heinz, Hildebrandt, Steffen, Struwe and Wente *et al.*

A solution is obtained provided that the original data is small with respect to the size of the boundary C. We state the classical theorem of existence due to Hildebrandt:

> *Let C be a Jordan curve included in a ball of radius $R > 0$. If $|H| \leq \frac{1}{R}$, there exists a topological disc spanning C and with mean curvature H* [23].

We should mention that the Hildebrandt result is the best possible one since we cannot drop the assumption on H: condition (4.4) shows that for H with $|H| > 1/R$, there does not exist a solution when C is a planar circle of radius R. There are many studies on the existence of solutions to the Plateau problem for CMC surfaces. The book by Struwe [68] and the survey paper [67] could serve as a lead for readers. Similarly, one can minimize the area functional for all disc-type surfaces spanning C and enclosing a fixed volume V. Of course, in the case where it is possible to obtain a minimum, the solution is a CMC surface. In this sense, we point out the following result of Wente [70]:

> *Given a Jordan curve C and a number $V > 0$, there exists a topological disc with constant mean curvature spanning C and enclosing a volume V.*

Although the above two results provide many CMC surfaces with boundary, no study has been done on the shape and morphology of these surfaces. Only in the case where C is a circle, is it known that the solution given by Hildebrandt is a spherical cap [5].

On the other hand, the isoperimetric problem can be stated as follows. Let C be a closed curve such that C is the boundary of a surface G. Given a positive number V, an *isoperimetric region with respect to* (G, V) is a region $M \subset \mathbb{R}^3$ of volume V such that $\partial M = G \cup \mathcal{S}$ and $\mathcal{S}$ has the least area among all the possible M. Existence of these isoperimetric regions is guaranteed in the context of the geometric measure theory [3]. From regularity, their boundaries are smooth except in C and so they give us embedded CMC surfaces, possibly of high genus.

However, in both problems, the geometry of the shapes of such surfaces is unknown.

Now assume that C is a planar curve. From experiments and for small volumes, one expects that the solutions obtained by Wente as well as the isoperimetric regions correspond with graphs on the domain determined by C. The mathematical proof of this evidence is in [49] when the boundary C is *convex*. The basic fact is the following estimate of the height of a CMC surface:

Theorem 4.1 ([49]). *Let $\mathcal{S}$ be a surface with constant mean curvature H. If $\partial\mathcal{S}$ is a closed curve included in a plane* Π, *then the height h of the surface with respect*

to Π *satisfies*

$$h \leq \frac{A|H|}{2\pi},$$

where A *is the area of the part of* $\mathcal{S}$ *that lies over* Π. *Equality holds if and only if* $\mathcal{S}$ *is a spherical cap.*

A consequence of this estimate is the description of Hildebrandt and Wente solutions for small volumes.

Theorem 4.2 ([43]). *Let* C *be a convex curve.*

(1) *There exists a value* $H_0(C) > 0$ *depending only on* C *such that Hildebrandt solutions are graphs if the mean curvature* H *satisfies* $|H| < H_0(C)$.
(2) *There exists a value* $V_0(C) > 0$ *depending only on* C *such that Wente solutions are graphs if the volume* V *satisfies* $V < V_0(C)$.

In the same way, Theorem 4.1 allows the shapes for some isoperimetric regions to be shown.

Theorem 4.3 ([49]). *Given a bounded convex planar domain* Ω, *there exists a positive number* V_Ω *such that isoperimetric regions with respect to the pair* (Ω, V) *for* $V \leq V_\Omega$ *are bounded by* $\Omega \cup \mathcal{S}$, *where* $\mathcal{S}$ *is a constant mean curvature graph over* Ω.

One question is what happens if the curve is not convex. We hope that the same result holds for arbitrary planar closed curves. This belief comes from the solvability of the CMC equation. If C is a planar closed curve, we know that for small values of H, there exist graphs with mean curvature H spanning C. An analysis of the mean curvature equation informs that in this range of H, the volume and the height are increasing functions on H [51]. Since the curve C is prescribed, we expect small volumes to correspond with droplets of high wettability. Thus, the droplet would actually be a graph.

4.2. *Existence of critical volumes*

When we increase the volume of the liquid deposited on the substrate, the configurations cease to be graphs and if the fluid rests pinned to the boundary C, the morphological wetting transitions can change completely. These transitions have been noted in the Max Planck Institute of Colloids and Interfaces at Golm in the study of chemically-structured surfaces containing hydrophilic and hydrophobic surfaces domains. These patterns are interesting in microfluidic devices, for example, in alkaness spreading, photolithography, copolymer films and vapor deposition. See [17] and references therein. It has been observed experimentally that the original cylinders on stripped domains change in an abrupt manner from a certain volume of liquid deposited on the substrate. See Fig. 6. The morphology of liquid is a function of the quantity of liquid injected along a given pattern. An addition of

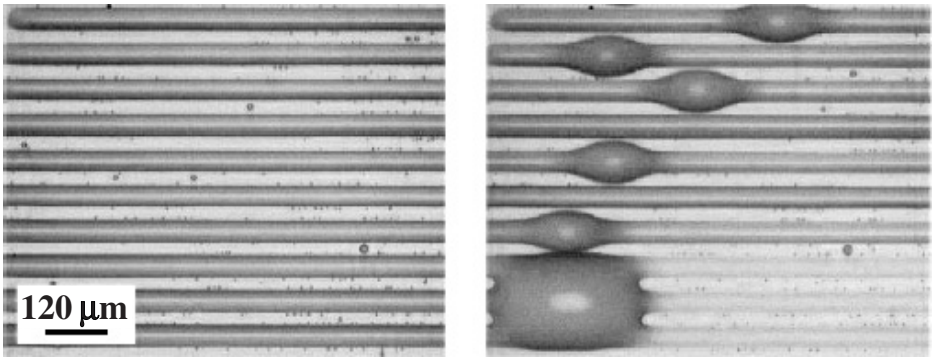

Fig. 6. Morphological wetting transitions of water channels on a hydrophilic MgF_2 striped surface. The effect of the volume on the shape of liquid appears at microscopic scale. When the amount of water is small, the shapes adopted are the expected ones as graphs on a band (left), i.e. pieces of cylinders. However, for a critical volume, the liquid develops bulges (right), even given the possibility of joining closer channels. Courtesy of R. Lipowsky.

volume produces bulges [17, 38]. Similar results have been noted for annular-type patterns [36].

In the same sense, different computing experiments developed at the GANG show similar situations. For a convex curve C, it seems that there exists a critical volume V_C with the following property: a CMC surface bounded by C and enclosing a volume $V > V_C$, has parts on both sides of Π [24]. Thus the existence of two wetting phenomena depending on the volume of fluid deposited on the substrate seems clear. If the volume is small, we know that the surface is a graph [49, 43]. But if we add liquid, the morphologies taken on by the droplet are unexpected.

The problem is also interesting for two convex curves C_1, C_2 in parallel planes. In this situation, if the volume V is small, isoperimetric regions are disconnected droplets deposited in each plane and such surfaces do not form a bridge between both planes. What happens when $V \to \infty$? We do not know the topology of the isoperimetric regions when the volume increases. Do the two droplets grow and touch for a first time, i.e. is there an isoperimetric region bounded by a topological cylinder joining C_1 to C_2? We do not even know if there is a constant mean curvature topological cylinder with boundary $C_1 \cup C_2$. The answer is affirmative only if C_1, C_2 are circles. In this case, if the droplet touches the planes in axially-concentric discs, then the surface is a rotational surface [42].

4.3. *Embedded CMC surfaces*

An *embedded* surface is a surface without self-intersections. For example, graphs of smooth functions are embedded. Although droplets obtained in experiments are embedded, mathematically a CMC surface can have self-intersections (an immersed surface). In this section, we assume that all the surfaces are compact. Shapes of embedded CMC surfaces are the best known due to the tangency principle.

Alexandrov used it in an original way to prove that *the only compact embedded CMC surfaces in* $\mathbb{R}^3$ *are round spheres* [2]. The proof is to compare the surface with itself (Alexandrov reflection method). The original question posed in Sec. 2 of whether a CMC surface inherits the symmetries of its boundary can be answered in some cases if we assume embedding on the surface. The best result in this sense is the following:

Theorem 4.4 ([29]). *Let* C *be a closed curve contained in a plane* Π. *Assume that* C *is symmetric with respect to a straight line* $L \subset \Pi$ *and that each piece of* C *that* L *divides is a graph on* L. *If* $\mathcal{S}$ *is an embedded CMC surface with boundary* C *and* $\mathcal{S}$ *lies on one side of* Π, *then* $\mathcal{S}$ *is symmetric with respect to plane* P *orthogonal to* Π *with* $P \cap \Pi = L$. *In particular, if* C *is a round circle, then* $\mathcal{S}$ *is a spherical cap.*

The proof consists of showing that $\mathcal{S}$ is invariant by symmetry with respect to P. Moreover, the proof shows that the parts of $\mathcal{S}$ in each side of P are graphs over a domain of P. For this, we work as follows. After an ambient isometry, we can suppose that $\Pi = \{z = 0\}$, $P = \{y = 0\}$ and $\mathcal{S} \subset \{z \geq 0\}$. Denote Ω the bounded region in Π bounded by $C = \partial\mathcal{S}$. Since $\mathcal{S} \cup \Omega$ is a closed surface, $\mathbb{R}^3 \setminus (\mathcal{S} \cup \Omega) = A \cup B$, being A and B non-bounded and bounded domains, respectively. We orient S by the Gauss map N that points towards A.

Consider the family of all translated copies of P given by $P(t) = \{y = t\}$ (hence $P(0) = P$). For t sufficiently negative, $P(t) \subset A$. Letting $t \to 0$, consider the first plane $P(t_1)$ that reaches $\mathcal{S}$, that is, $P(t_1) \cap \mathcal{S} \neq \emptyset$ but $P(t) \cap \mathcal{S} = \emptyset$ if $t < t_1$. Now, when we increase t from t_1, we denote by $\mathcal{S}(t)^-$ and $\mathcal{S}(t)^+$ the (closed) parts of $\mathcal{S}$ on the left and right of $P(t)$, respectively. Let $S(t)^*$ be the symmetry of $\mathcal{S}(t)^-$ through $P(t)$. Initially, when we take t sufficiently close to t_1 with $t > t_1$, $\mathcal{S}(t)^*$ is contained in B and $\mathcal{S}(t)^*$ and $\mathcal{S}(t)^-$ are graphs on $P(t)$. As t continues to increase, and through the compactness of $\mathcal{S}$, there exists a critical time τ, $\tau > t_1$, such that $\mathcal{S}(\tau)^*$ has a first contact with $\mathcal{S}(t)^+$, that is, $\mathcal{S}(\tau) \subset B$ and there exists $p \in \mathcal{S}(\tau)^* \cap \mathcal{S}(\tau)^+$ at which, for $t > t_1$ $\mathcal{S}(t)^*$ leaves to be contained in B. Different possibilities may occur. First, if $\tau = 0$, then $\mathcal{S}(0)^* \subset B$. In this case, we repeat the argument but we begin from $t = \infty$. We continue with the reasoning below. If we can once again arrive, by carying out reflection, at the position $t = 0$, then P is a plane of symmetry of $\mathcal{S}$. In other case, our reasoning is similar to the one below.

On the contrary case, $\tau < 0$ and there exists $p \in \mathcal{S}(\tau)^*$ such that the tangent planes of $\mathcal{S}(\tau)^*$ and $\mathcal{S}(\tau)^+$ are equal at p. See Fig. 7. The point p may be an interior or boundary point of $\mathcal{S}(\tau)^*$ but it is prohibited that $p \in C$, due to the symmetry of C and the fact that $\mathcal{S}$ lies over Π. Now we will consider $\mathcal{S}(\tau)^*$ and $\mathcal{S}(\tau)^+$ graphs with respect to $T_p\mathcal{S}$. In addition, the Gauss maps of both surfaces at p agree since $\mathcal{S}$ is embedded. Applying the tangency principle (in both interior or boundary versions), we conclude that $\mathcal{S}(\tau)^* = \mathcal{S}(\tau)^+$ and $P(\tau)$ is a plane of symmetry of $\mathcal{S}$, in contradiction with the symmetry of C with respect to L.

Theorem 4.4 generalizes in two senses. Let us first consider a CMC embedded surface bounded by two coaxial circles. We know that if the surface is included in the

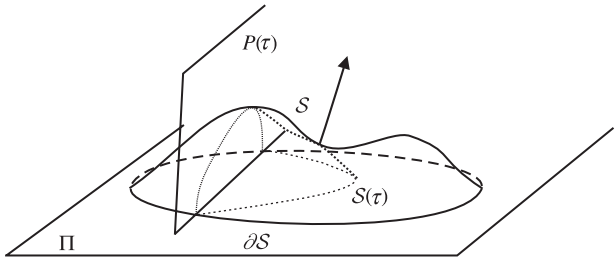

Fig. 7. The Alexandrov reflection method.

slab determined by the two boundary planes, the surface is rotationally symmetric [42]. What happens if the surface exceeds this slab? Pieces of nodoids show the existence of CMC rotational symmetric surfaces spanning two coaxial circles, but the surface is not included in the slab determined by the boundary.

Q3 Let $\mathcal{S}$ be a CMC embedded surface bounded by two coaxial circles. Is $\mathcal{S}$ a surface of revolution?

On the other hand, Theorem 4.4 is generalized for more general assumptions on the mean curvature. If we think a droplet as an embedded surface resting on a planar substrate under the effect of the gravity that makes a constant angle of contact with the planar substrate, a theorem of Wente shows that the droplet is rotational symmetric with respect to a straight line orthogonal to Π [71]. Furthermore, each intersection of the droplet with a horizontal plane is a round circle. In fact, this result is key for experimentalists since it is a custom to consider rotational symmetric droplets. However, even for minimal surfaces, there are immersed counter-examples. Recall also that Kapouleas found non-embedded CMC surfaces spanning a circle.

More recently, we pointed out two results that inform us how the geometry of the boundary has an effect on the whole surface. We give a quick proof of them without going into details.

Theorem 4.5 ([29]). *Let C be a Jordan curve included in a plane Π and let us denote Ω the domain bounded by C. Let $\mathcal{S}$ be an embedded CMC surface spanning C. If $\mathcal{S}$ does not intersect $\Pi\backslash\bar{\Omega}$, then $\mathcal{S}$ lies on one side of the half-spaces determined by Π. In particular, if C is a circle, $\mathcal{S}$ is a spherical cap.*

We assume that $\mathcal{S}$ has points on both sides of Π. We take a large lower hemisphere Q such that the disc that bounds ∂Q in Π contains ∂C and $Q \cap \mathcal{S} = \emptyset$. Then $Q \cup \mathcal{S}$ together with the annulus determined by ∂Q and C is a closed surface in $\mathbb{R}^3$ that encloses a domain W. See Fig. 8. We orient $\mathcal{S}$ by the Gauss map N that points towards W. We use the touching principle to compare $\mathcal{S}$ with that horizontal plane at the lowest point p of $\mathcal{S}$ to infer that $H < 0$. On the other hand, at the highest point q of $\mathcal{S}$, a new comparison with the tangent plane gives $H > 0$, which is a contradiction.

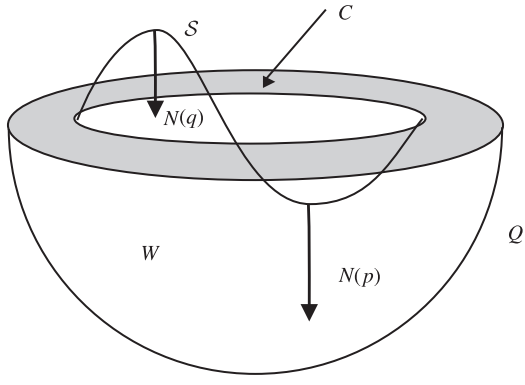

Fig. 8. Proof of Theorem 4.5.

Theorem 4.6 ([8]). *Let C be a convex curve included in a plane Π. Let $\mathcal{S}$ be an embedded CMC surface spanning C. If $\mathcal{S}$ is transverse to Π along C, then $\mathcal{S}$ lies in one side of Π. In particular, if C is a circle, $\mathcal{S}$ is a spherical cap.*

Here we show two cases that can illustrate the proof of this result. In Fig. 9(a), the surface meets the plane Π in a nullhomotopic closed curve G in $\Pi \backslash \Omega$. We use the Alexandrov reflection method by vertical planes arriving from infinity. Since C is convex, we would have an interior contact point, proving that $\mathcal{S}$ has a symmetry by a vertical plane that does not intersect C: this case is impossible.

The second case that we analyze appears in Fig. 9(b). Again, this surface is impossible. In this situation, we use the balancing formula as follows. The surface $\mathcal{S}$ together with Ω encloses a domain W and we orient $\mathcal{S}$ by N pointing towards W. Here the mean curvature H is positive. Set $\vec{a} = (0, 0, 1)$. In the expression (4.2), $\langle \nu, \vec{a} \rangle$ is positive, since the surface is transverse to Π along $\partial \mathcal{S}$. Since $\alpha' = \nu \wedge N$, the term $\langle \alpha \wedge \alpha', \vec{a} \rangle$ is also positive, which is again a contradiction.

It is possible to add to Theorem 4.6. If the droplet is a graph around the boundary, the surface is actually a graph:

Theorem 4.7 ([41]). *Let C be a Jordan curve included in a plane Π and let Ω be the domain that bounds in Π. Let $\mathcal{S}$ be an embedded CMC surface spanning C. If $\mathcal{S}$ is a graph over Ω around the boundary C, then the surface is a graph.*

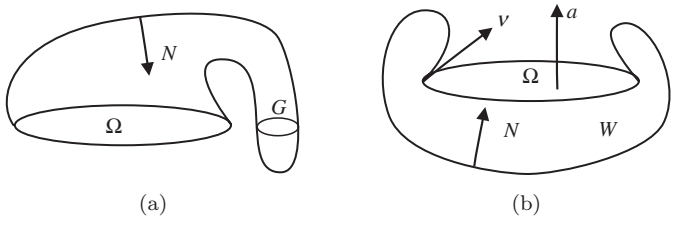

Fig. 9. Proof of Theorem 4.6.

In this result, we again use the Alexandrov reflection method but with horizontal planes: let us consider $Q = \mathcal{S} \cup (C \times [-\infty, 0])$ and B the domain of $\mathbb{R}^3 \setminus Q$ that contains Ω. Let us orient $\mathcal{S}$ by the Gauss map that point towards B. Carrying out the Alexandrov reflection method with horizontal planes coming from infinity, there are two possibilities: there exists a contact position between an interior point p of $\mathcal{S}$ with a point q of C; or we can carry on doing reflections with planes until arriving at Π. In the former case, there is a contradiction because $\mathcal{S}$ is a graph on Ω around C but the segment joining p with q must be in B. As a consequence, the second possibility occurs, proving that $\mathcal{S}$ is a graph.

From this result, consider C a closed curve included in a plane Π and let $\mathcal{S}$ be an embedded CMC surface spanning C such that $\mathcal{S}$ lies over Π. We know that for small volumes, $\mathcal{S}$ is a graph, but we do not know if the same occurs when the height of $\mathcal{S}$ is not very great. The height of an embedded surface is controlled as follows. Consider an embedded compact surface $\mathcal{S}$ with constant mean curvature H. Assume that $\partial\mathcal{S}$ is contained in a plane Π and $\mathcal{S}$ lies in one of the two half-spaces determined by Π. A similar reasoning with the Alexandrov reflection method as in Theorem 4.4 but using horizontal planes coming from infinity, we can easily show that there is no contact point in the reflection process at least until the height $h/2$, being h the height of $\mathcal{S}$. Since until this moment, the part of surface behind the plane at height $h/2$ is a graph, we conclude the following.

The maximum height of an embedded compact surface with mean curvature H, planar boundary and above the boundary plane is $2/|H|$.

This estimate is optimal for big spherical caps.

Q4 Big spherical caps are not graphs. Thus, we ask if an embedded surface with constant mean curvature H, planar boundary and with height $1/|H|$ not far from the boundary plane is actually a graph? Furthermore, we expect $\mathcal{S}$ to be a hemisphere if the height attains the value $1/|H|$.

Finally, we ask about the topology of a CMC droplet resting over a plane. One open question is whether an embedded CMC surface with convex boundary and over the plane containing the boundary has the same topology as a disc [8]. We know that this is true in some cases: see Theorems 4.3 and 4.7. If the case of small volume was treated in [49], Ros and Rosenberg have proved an analogous result if the volume is so big.

Theorem 4.8 ([61]). *Let C be a convex curve included in a plane Π. There exist numbers V_0 and A_0, depending only on C, such that any embedded CMC surface with boundary C and over Π is a topological disc provided that either its volume or area is bigger than V_0 and A_0 respectively.*

The authors have also proved that for large volumes (or areas), the surface is like a sphere. In particular, the surface is the union of two graphs: first, over the domain D that contains Ω, the domain that bounds C on Π, together with a graph

on the annulus $D \setminus \Omega$. We expect this to be true with the only assumption that surface $\mathcal{S}$ is locally a graph over $\Pi \setminus \Omega$ around C. Physically, this means that $\mathcal{S}$ *dewets* along C.

Q5 Is there a domain D with $\bar{\Omega} \subset D$ such that $\mathcal{S} = \mathcal{S}_1 \cup \mathcal{S}_2$, being $\mathcal{S}_1$ and $\mathcal{S}_2$ graphs over D and $D \setminus \bar{\Omega}$ respectively?

4.4. *CMC surfaces with circular boundary*

Returning to the case of circular boundary, the first example is a spherical cap. If we cut off a sphere by a plane, we obtain two surfaces with the same circle as a boundary, i.e. hemispheres, if the plane crosses the center of the sphere, or two (different) spherical caps. However, our mathematical CMC droplets can have configurations that are physically unrealizable. Even in the simple case that the surface has the same topology as a disc or it has no self-intersections, non-spherical shapes of droplets could appear. Definitively, are the droplets on circular domains round?

If the radius of the circle is R, a necessary condition about the value of H is that $|H| \leq 1/R$ ([22] and formula (4.2)). In this case, the only known examples are the planar disc ($H = 0$), the two corresponding spherical caps of radius $1/|H|$ if $H \neq 0$, and the Kapouleas examples [28] cited in Sec. 2. However, computers have no numerical images of these surfaces.

We report here recent results that characterize spherical caps in the family of CMC surfaces with circular boundary.

Theorem 4.9. *Let C be a circle of radius R and let $\mathcal{S}$ be a compact surface spanning C and with constant mean curvature H. Then, $\mathcal{S}$ is a spherical cap if one of the following conditions holds*:

(1) *The surface is embedded and lies over the plane containing C* [2].
(2) *The surface is embedded and do not intersect the exterior domain of the circle in the boundary plane* [29].
(3) *The mean curvature satisfies $|H| = 1/R$* [7].
(4) *The surface is included in a closed ball of radius $1/|H|$* [5].
(5) *The surface is embedded and transverse to the boundary plane along the boundary* [8].
(6) *The surface is a minimizer surface* [30].
(7) *The surface is a topological disc with an area less than the area of the small spherical cap with mean curvature H* [48].
(8) *The volume is less than the volume of a hemisphere* [49].
(9) *The surface is embedded and included in a slab of width $1/|H|$* [40].
(10) *The surface is a stable topological disc* [4].

(11) *The surface is a topological disc that makes a constant angle of contact along the boundary* [43].
(12) *The surface is stable and with a free boundary along the boundary plane* [31].

5. Conclusions and Outlook

Constant mean curvature surfaces with prescribed boundary are models for interfaces in a microgravity environment or a microscopic scale. Experiments under non-ideality conditions show that the condition concerning the contact angle is not satisfied (hysteresis). When we deposit a sufficient amount of liquid on a heterogeneous substrate, interfaces are constrained to the borders that separate hydrophilic and hydrophobic domains. If the volume of liquid, or the contact angle, is small (wetting), mathematical results show that CMC graphs simulate the adopted shapes reasonably well. For convex domains at least, the results reported here reveal a mathematical activity on the existence of the Dirichlet problem. This suggests that a major emphasis can be addressed to experiment with shapes for liquids in a non-parametric surface $z = f(x, y)$. It would be of interest to study the relationship between the size of the substrate surface with the construction of liquid droplets, their heights and volumes.

Advances in computer technology open the possibility of modeling solutions of the Dirichlet problem. On the other hand, and in the light of the results of the literature, the control of the relation between the shape of the interface and the amount of liquid that contains is not completely understood, since, for large volumes, the interface leaves to be a graph and the morphologies observed are unexpected. In this situation, the shapes obtained experimentally show how the models of such systems are far from being understood.

Finally, one comment. The points of view of a physicist and a mathematician can converge, as for example, when experiments in wetting and capillarity help to reach the results that a mathematician is attempting to prove and vice versa; that is, how mathematics provides a model for a physical phenomenon that allows a relative description of these morphologies. However, just as has been shown throughout these pages, one thing is the experimental evidence and another is the theoretical proof. The conjecture on spherical caps (see Sec. 2) is an example of this complexity. The richness of the space of CMC surfaces with boundary and the variety of shapes of such surfaces goes well beyond the limits of the experience: surfaces that are probably physically unrealizable but mathematically possible.

Acknowledgments

The author would like to thank the referees for reading the paper carefully while providing suggestions and comments to improve it. This work has been partially supported by a MEC-FEDER grant no. MTM2004-00109.

References

[1] A. W. Adamson, *Physical Chemistry of Surfaces* (John Wiley and Sons, New York, 1990).
[2] A. D. Alexandrov, *V. Vestnik Leningrad Univ. A.M.S. Ser. 2*, **21** (1958) 412.
[3] F. J. A. lmgren, *Mem. Amer. Math. Soc.* **4** (1976).
[4] L. Alías, R. López and B. Palmer, *Proc. A.M.S.* **127** (1999) 1195.
[5] J. L. Barbosa, *Matem. Comtemp.* **1** (1991) 3.
[6] K. Brakke, *Exp. Math.* **1** (1992) 141.
[7] F. Brito and R. Earp, *An. Acad. Bras. Ci.* **3** (1991) 5.
[8] F. Brito, R. Earp, W. Meeks III and H. Rosenberg, *Indiana Univ. Math. J.* **40** (1991) 333.
[9] P. Collin, *C.R. Acad. Sci. Paris Sér. I* **311** (1990) 539.
[10] R. Courant and D. Hilbert, *Methods of Mathematical Physics* (Interscience, New York, 1962).
[11] C. Delaunay, *J. Math. Pure et App.* **16** (1841) 309.
[12] N. Espirito-Santo and J. Ripoll, *J. Geom. Anal.* **11** (2001) 603.
[13] R. Finn, *J. d'Anal. Math.* **14** (1965) 139.
[14] R. Finn, *Equilibrium Capillary Surfaces* (Springer-Verlag, New York, 1986).
[15] R. Finn, *J. Math. Fluid Mech.* **3** (2001) 139.
[16] P. Fusieger and J. Ripoll, *Ann. Global Anal. Geom.* **23** (2003) 373.
[17] H. Gau, S. Herminghauss, P. Lenz and R. Lipowsky, *Science* **283** (1999) 46.
[18] K. F. Gauss, *Comment. Soc. Regiae. Scient. Gottingensis Rec.* **7** (1830), reprinted in Werke, Vol. 5 (Gottingen, 1876), 29.
[19] J. Gaydos, *Colloids and Surfaces A: Physicochemical and Engineering Aspects* **114** (1996) 1.
[20] P. G. deGennes, F. Brochard-Wyart and D. Quéré, *Capillarity and Wetting Phenomena: Drops, Bubbles, Pearls, Waves* (Springer-Verlag, New York, 2004).
[21] D. Gilbarg and N. S. Trudinger, *Elliptic Partial Differential Equations of Second Order* (Springer-Verlag, New York, 1983).
[22] H. Heinz, *Arch. Rational Mech. Anal.* **35** (1969) 249.
[23] S. Hildebrandt, *Commun. Pure Appl. Math.* **23** (1970) 97.
[24] D. Hoffman and H. Rosenberg, *Surfaces Minimales et Solutions de Problmes Variationnels* (Soc. Math. France, Paris, 1993).
[25] J. T. Hoffman, MESH: A program for generating parametric surfaces using an adaptive mesh, Document Library, Series 2, No. 35, Univ. Massachusetts (1995).
[26] E. Hopf, *Preuss. Akad. Wiss.* **19** (1927) 147.
[27] R. E. Johnson and R. H. Dettre, *Surface Coll. Science* **1** (1969) 85.
[28] N. Kapouleas, *J. Diff. Geom.* **33** (1991) 683.
[29] M. Koiso, *Math. Z.* **191** (1986) 567.
[30] M. Koiso, *Manuscripta Math.* **87** (1995) 311.
[31] M. Koiso, *Bull. Kyoto Univ. Ed. Ser.* **B94** (1999) 1.
[32] R. Kusner, Global geometry of extremal surfaces in three-space, Ph.D. thesis, Univ. California, Berkeley, 1998.
[33] D. Langbein, *Microgravity Sci. Technol.* **5** (1992) 2.
[34] D. Langbein, *Capillary Surfaces* (Springer-Verlag, Berlin, 2002).
[35] P. S. Laplace, *Traité de la Mecánique Celeste; Supplements en livre X* (Gauthier-Villais, Paris, 1806).
[36] P. Lenz, W. Fenzl and R. Lipowsky, *Europhys. Lett.* **53** (2001) 618.
[37] G. Lian, C. Thornton and M. Adams, *J. Coll. Interface Sci.* **161** (1993) 138.
[38] R. Lipowsky, *Current Op. Colloid Interface Sci.* **6** (2001) 40.

[39] S. Ljunggren, J. C. Eriksson and P. A. Kralchevsky, *J. Coll. Interfaces Sci.* **191** (1997) 424.
[40] R. López, *Geom. Dedicata* **66** (1997) 255.
[41] R. López, *J. Geom.* **60** (1997) 80.
[42] R. López, *Ann. Global Anal. Geom.* **15** (1997) 201.
[43] R. López, *Tsukuba J. Math.* **23** (1999) 27.
[44] R. López, *J. Diff. Eq.* **171** (2001) 54.
[45] R. López, *Pacific J. Math.* **206** (2002) 359.
[46] R. López, *Glasgow Math. J.* **44** (2002) 455.
[47] R. López, *Manuscripta Math.* **110** (2003) 45.
[48] R. López and S. Montiel, *Proc. A. M. S.* **123** (1995) 1555.
[49] R. López and S. Montiel, *Duke Math. J.* **85** (1996) 583.
[50] U. M. Marconi and F. Van Swol, *Phys. Rev.* **A39** (1989) 4109.
[51] J. McCuan, *Calc. Var.* **9** (1999) 297.
[52] A. W. Neumann and J. K. Spelt, *Applied Surface Thermodynamics* (Marcel Dekker, New York, 1996).
[53] J. C. C. Nitsche, *Lectures on Minimal Surfaces* (Cambridge University Press, Cambridge, 1989).
[54] R. Osserman, *A Survey of Minimal Surfaces* (Dover Publ. Inc., New York, 1986).
[55] A. O. Parry, C. Rascón and A. J. Wood, *Phys. Rev. Lett.* **85** (2000) 345.
[56] L. E. Payne and G. A. Philippin, *Nonlinear Anal. Theory Meth. App.* **3** (1979) 193.
[57] D. Queré, *Physica* **A313** (2002) 32.
[58] C. Rascón and A. O. Parry, *Nature* **407** (2000) 986.
[59] J. Ripoll, *Pacific J. Math.* **198** (2001) 175.
[60] J. Ripoll, *J. Differential Equations* **181** (2002) 230.
[61] A. Ros and H. Rosenberg, *J. Diff. Geom.* **44** (1996) 807.
[62] A. Ros and H. Rosenberg, Properly embedded surfaces with constant mean curvature, preprint (2004).
[63] P. R. Rynhart and R. McLachlan, J. R. Jones and R. McKibbin, *Res. Lett. Inf. Math. Sci.* **5** (2003) 19.
[64] L. L. Schramm, D. B. Fisher, S. Scürch and A. A. Cameron, *Colloids Surf.* **A94** (1995) 145.
[65] J. Serrin, *Philos. Trans. Roy. Soc. London Ser.* **A264** (1969) 413.
[66] J. Serrin, *Math. Z* **11** (1969) 77.
[67] K. Steffen, *Lecture Not. Math.* **1713** (1999) 211.
[68] M. Struwe, *Plateau's Problem and the Calculus of Variations* (Princeton Univ. Press, Princeton, 1988).
[69] M. E. Urso, C. J. Lawrence and M. J. Adams, *J. Colloid Int. Sci.* **220** (1999) 42.
[70] H. C. Wente, *J. Math. Anal. Appl.* **26** (1969) 318.
[71] H. C. Wente, *Pacific J. Math.* **88** (1980) 387.
[72] T. Young, *Philos. Trans. Royal Soc.* (London) **1** (1805) 65.